

The influence of structure changes in the properties of TiC_xO_y decorative thin films

A.C. Fernandes ^{a,*}, F. Vaz ^a, L. Cunha ^a, N.M.G. Parreira ^b, A. Cavaleiro ^b, Ph. Goudeau ^c, E. Le Bourhis ^c, J.P. Rivière ^c, D. Munteanu ^d, B. Borcea ^d, R. Cozma ^e

^a Universidade do Minho, Dept. Física, Campus de Azurém, 4800-058 Guimarães, Portugal

^b ICMES — Fac. Ciências e Tecnologia Universidade de Coimbra, 3030-201 Coimbra, Portugal

^c Laboratoire de Métallurgie Physique, Université de Poitiers, 86960 Futuroscope, France

^d Department of Technological Equipment and Materials Science, Transilvania University, 29 Eroilor Blvd., 500036 Brasov, Romania

^e Department of Product Design and Robotics, Transilvania University, 29 Eroilor Blvd., 500036 Brasov, Romania

Received 3 January 2006; received in revised form 4 January 2007; accepted 16 January 2007

Available online 24 January 2007

Abstract

The main purpose of this work consists in the preparation of titanium oxycarbide, TiC_xO_y , thin films, in which the presence of oxygen changed the film properties between those of titanium carbide and those of titanium oxide. Varying the oxide/carbide ratio allowed to tune the structure of the films between titanium oxide and carbide and consequently electronic, mechanical and optical properties of the films. The depositions were carried out from a TiC target by direct current, dc, reactive magnetron sputtering, varying the oxygen flow rate. The obtained results showed that the film's properties can be divided into 3 different regimes — i) carbide, ii) a transition zone and iii) an oxide one. X-ray diffraction results revealed the occurrence of a face-centered cubic phase (TiC-type) for low oxygen content, also obtained in the $\text{TiC}_{1.6}(\text{O})$ film, with a clear tendency towards amorphization with the increase of the oxygen flow rate. For the highest oxygen contents, the results revealed the development of a mixture of poorly crystallized TiO_2 phases. The colour results indicated a strong dependence on the O/Ti ratio. A progressive reduction of hardness and residual stresses with the increase of the O/Ti ratio was also observed. The residual stresses, as well as the film structure, seem to play an important role on the adhesion of the coatings. The static friction coefficient revealed also some correlation with the mechanical properties, but mainly with the surface roughness.

© 2007 Elsevier B.V. All rights reserved.

PACS: 68.55.Jk; 68.55.Ln; 68.55.Nq; 68.60.Bs; 78.20.Ci; 78.66.Sq; 81.15.Aa; 81.15.Cd

Keywords: TiC_xO_y coatings; X-ray diffraction; Phase transitions; Decorative films; Hardness

1. Introduction

Transition metal carbides, such as TiC, form a class of very hard materials and often crystallize in the rock salt structure. They show metallic as well as covalent and ionic properties, exhibiting a unique combination of characteristics that allow them to be serious candidates for a wide range of high-technology applications [1–6]. Beyond these technological applications that can range from several examples in metallurgy, aeronautics, electronics and medicine, used to protect and to decrease wear in a variety of components, there is also the more

specific case of fundamental research, where these carbides have been revealed to be a subject of great interest [7,8]. The wide structural features revealed with, for instance, the variation of the C content, is one of the factor that is interesting for the research teams [1–6]. While exhibiting a number of unusual properties, most applications of the transition-metal carbides rely upon their extreme hardness, which are typically found for covalent crystals [9].

Carbide films can be deposited by a variety of chemical vapour deposition (CVD) and physical vapour deposition (PVD) techniques [8,10–15]. Usually the CVD methods are limited owing not only to environmental problems, but also to the high temperatures involved during processing. Among the PVD methods, sputtering is one of the most commonly used.

* Corresponding author. Tel.: +351 253510475; fax: +351 253510461.

E-mail address: acrist@fisica.uminho.pt (A.C. Fernandes).

However, during sputter deposition it is difficult to maintain the appropriate parameters of deposition in order to obtain the desirable film properties such as stoichiometry, structure, hardness, colour, etc., although, this technique permits the manipulation of a lot of parameters such as deposition energy (bias), deposition rate (plasma current), reactive to neutral gas concentration in plasma, etc. When dealing with reactive gases, these problems are even more serious.

Nevertheless, the increasing need to have multifunctional materials, with properties that become better and better suitable for a certain application, have prompted the investigations in this field of materials science, and the addition of a third element is often seen as one of the most successful approaches. In this respect, the addition of oxygen to the Ti–C matrix is one of the possibilities that can be seen as generating a wide spread of properties. In fact, the presence of oxygen on TiC films allows the tailoring of film properties between those of metal carbides, as the case of TiC, and those of the correspondent large ionic oxides, with the consequent wide variation in the materials' properties. Thus, the main purpose of this work is to present experimental results on the influence of oxygen additions to Ti–C films and to advance a qualitative explanation for the development of the different structural arrangements. Special attention will be given to the formulation of a simple explanation, which explains the revealed behaviour concerning the growth modes and the evolution of the film's mechanical and tribological properties.

2. Experimental details

The TiC_xO_y films were deposited by reactive dc magnetron sputtering, from a TiC target onto polished high-speed steel (AISI M2), (100) single crystalline silicon wafers and stainless steel (AISI 316) substrates. The substrates were ultrasonically cleaned and in-situ sputter etched for 15 min in a 0.15 Pa Ar atmosphere. The depositions were carried out in a laboratory-size magnetron sputtering deposition system. The films were prepared with the substrate holder positioned at 70 mm in all runs, applying a direct current (d.c.) density of 0.5 A, corresponding to a TiC target current density of 25 A m^{-2} . A gas atmosphere composed of argon (working gas) and oxygen was used. The Ar flow was kept constant at 60 sccm and the oxygen flow varied from 0.5 to 3.5 sccm, corresponding to a partial pressure variation from 7.8×10^{-3} to 3.2×10^{-2} Pa. The working pressure was kept approximately constant at 4×10^{-1} Pa and the substrates were grounded and placed in static position during the depositions.

The atomic composition of the as deposited samples was measured by electron probe microanalysis in a Cameca SX-50 apparatus. The crystallographic structure was investigated by X-ray diffraction (XRD) in the Bragg–Bretano configuration, using monochromatic Cu $K\alpha$ radiation. A Digital Instruments NanoScope III atomic force microscope, working in tapping mode, was employed to study the surface morphology of these coatings. Film's colour was computed using a commercial MINOLTA CM-2600d portable spectrophotometer (wavelength range: 400–700 nm), using diffused illumination at an

8° viewing angle. The spectrophotometer was equipped with a 52 mm diameter integrating sphere and 3 pulsed xenon lamps. Colour specification was computed under the standard CIE illuminant D65 (specular component excluded) and represented in the CIELAB 1976 colour space [16,17]. Residual stresses, σ_r , were obtained from the substrates curvature, using Stoney's equation [18]. Film's hardness and Young's modulus were determined from the loading and unloading curves, carried out with an ultra low load-depth sensing Berkovich nanoindenter from CSM Instruments (Switzerland). The maximum load used was 30 mN, with a loading time of 30 s, holding 30 s and unloading in 30 s, producing an average number of 15 indentations per sample.

The adhesion/cohesion of the coatings was evaluated by scratch-testing technique using a Revetest, from CSM Instruments. The load was increased linearly from 0 to 50 N (Rockwell C 200 μm radius indenter tip, loading speed of 100 N/min, and scratch speed of 10 mm/min). The L_C values (normally known as L_{C2}), corresponding to the adhesive failure mechanisms were measured by analyzing the failure events in the scratch track by optical microscopy.

The static friction coefficient values, μ_s , were established by the inclined plan slope method. This method can estimate the μ_s based on typical linear size measurements involving the correction between the friction angles, α , and the static friction coefficient, μ_s , according the following ($\tan\alpha = \mu_s$). For each sample, using different friction conditions (plane fixed half-couple manufactured by heat treatable steel (AISI B7), in annealing heat-treatment conditions with three different roughness values, R_z , between 0.4 and 2.5 μm). The work with different roughness values of fixed plane half-couple is important in order to take into consideration the possible influence of sliding — plane roughness on friction process and to have an average value of static friction coefficient. Before the tribological tests, the samples were first degaussed and then alkaline cleaned and wiped. The fixed half-couple was also degaussed and periodically alkaline cleaned and wiped. According to the method description, 10 friction tests were performed for each sample on each half-couple: 5 in one direction and 5 abeam, in order that the one-way roughness could not influence the moving of the samples. In each case, the utmost values were eliminated. The environmental conditions of tribological tests were: $T=23.5 \text{ }^\circ\text{C}$ and 63% humidity.

3. Results

Table 1 shows a summary of all films prepared within the framework of this paper, together with their composition, as well as the correspondent thickness. From the table results, it is clear that as the oxygen flow increases, the atomic concentration of C decreases, the atomic concentration of O increases and the atomic concentration of Ti suffers only slight variations, within the range of 22 and 32 at.%. These variations can also be seen in Fig. 1a), where the ternary plot of the prepared samples within the Ti–C–O system is presented. Important to note is also the variation of the atomic ratio O/Ti, Fig. 1b), that will be used throughout the text as indicative of influencing film properties

Table 1
Thickness and composition of the prepared samples

Sample	Oxygen flow (sccm)	Ti (at.%)	C (at.%)	O (at.%)	O/Ti	Thickness (μm)
TiC _{1.3} O _{0.8}	0.5	32.1	41.4	26.5	0.8	0.9 \pm 0.1
TiC _{1.3} O _{1.1}	1.0	28.8	38.2	33.0	1.1	1.5 \pm 0.1
TiC _{0.9} O _{1.6}	1.5	28.2	25.9	45.9	1.6	1.4 \pm 0.1
TiC _{0.2} O _{1.8}	2.0	33.2	6.8	60.0	1.8	1.2 \pm 0.1
TiC _{0.1} O _{2.6}	2.5	27.3	2.5	70.2	2.6	1.0 \pm 0.1
TiC _{0.1} O _{3.4}	3.5	22.6	1.6	75.8	3.4	0.6 \pm 0.1

variations. Fig. 1b) shows that this atomic ratio increases almost linearly with the increase of the oxygen flow, which might be an indication of Ti target poisoning, as already noticed [11]. Taking into account the different element compositions, this diagram can be divided into 3 multiphase regions with the increase of the oxygen flow: i) a region I — where the films were prepared in the carbide regime; ii) a transition regime — region T, where the films were prepared with the conditions between those of carbide and those of oxide regimes, which it will be noted in the text as T; iii) region II — oxide zone.

Within region I, the films have relatively high amounts of C, with concentrations between ~ 41 and ~ 26 at.% (including the “pure” TiC_x(O) sample). The Ti concentration is almost constant with a value close to 30 at.%, and the O content increases from about 5 (contamination in the TiC_x sample) to about 46 at.%. The T region corresponds to a transition mode, which can be associated to the transition regime between the carbide and compound (oxide) regime in the hysteresis cycle of carbides [19]. The samples prepared within this regime have an atomic ratio O/Ti between 1.8 and 2.6. For region II, the C content is very low (< 5 at.%), while O has its highest values (> 70 at.%). Within this oxide region, the Ti concentration decreases slightly to ~ 23 at.% and thus, the formation of oxides is dominant as shown in the structural characterization presented in Fig. 2. The samples concerning this region presented an atomic ratio O/Ti ≥ 3 .

XRD patterns for samples prepared within the different sputtering modes are shown in Fig. 2. The results revealed that each of the different growth modes corresponded to different structural arrangements. Region I, which is related to the films that were grown in the metallic mode, developed a crystalline structure that is indexed to a fcc type, typical for TiC ($a_0 = 0.43274$ nm [20]). The same type of structure can also be observed for the TiC film, TiC_{1.6}, which is an interesting result since the carbon content is relatively high. This relatively high carbon content induces that in this particular TiC film, prepared in the same conditions used for the TiC_xO_y films, there might be also an amorphous carbon phase in the grain boundaries of the TiC grains, forming a composite of the type nc-TiC/a-C, as claimed by several authors [21–23]. An oxygen contamination amount between 1 and 5 at.% is also to be admitted in this sample. Moreover, a closer look to the diffraction patterns reveals that there is some tendency for the increase of the peak intensity ratio $I_{(200)}/[I_{(111)} + I_{(200)}]$ towards values typical of randomly oriented films, with the increase of the O/Ti ratio. Also, some tendency to the decrease of grain size with the increase of the O/Ti ratio can be claimed by the

significant peak broadening revealed by the film prepared with 0.5 sccm oxygen flow (O/Ti=0.8) when compared to the TiC_{1.6}(O) film. This growth of an amorphous oxide phase would, in fact, be consistent with this grain size reduction.

The results obtained for the zone T revealed an extensive tendency to amorphization of the films. In this region, the carbon content is significantly reduced and the amount of oxygen is already relatively high, which might be a sign of some difficulties to form carbide phases and thus enhancing the tendency to prepare amorphous films. For higher O/Ti ratios, the obtained structures consisted in oxide phases (a mixture of anatase and rutile), which in fact might be expected due to the very high O/Ti ratio and very low C content. Furthermore, and due to the very reduced amounts of C, it is also necessary to take into account the possibility to have some carbon in these oxides structures or within the grain boundaries or even in some amorphous carbide structures (possibly oxygen-doped ones).

These three distinct behaviours occurring within the different zones can also be correlated with the film’s colour characterization, Fig. 3. This figure shows the colour coordinates L^* , a^* and b^* , represented in the CIELAB (1976) colour space [16,17]. It can be observed that with increasing O/Ti atomic ratio (up to ~ 1.2), the value of a^* (redness) increases as well as

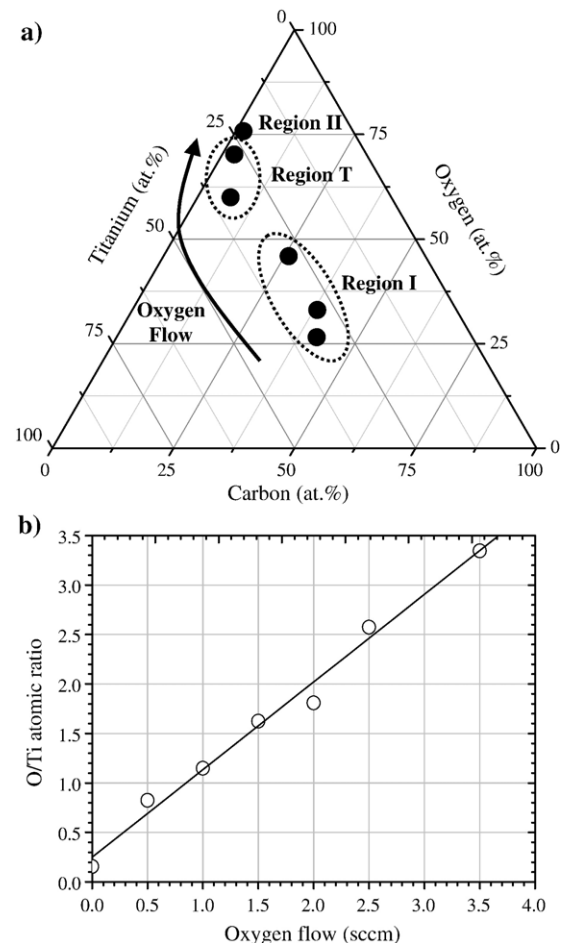


Fig. 1. (a) Ternary plot of the prepared samples within TiC_xO_y system. (b) Variation of O/Ti ratio with oxygen flow.

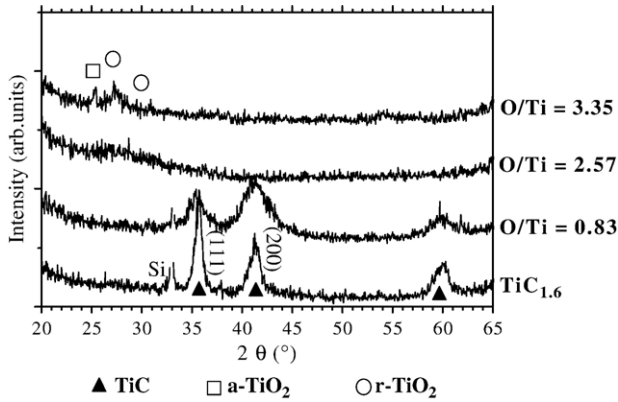


Fig. 2. X-ray diffractograms of TiC_xO_y films for different O/Ti ratio.

the b^* value (yellowness), reaching its maximum value. The L^* values (brightness) show a significant decrease for the Ti–C–O films with the increase of O/Ti ratio up to O/Ti ~ 1.8 . The colour changes from a metallic tone for the lowest O/Ti ratios (also for the $TiC_{1.6}(O)$ film) to a very bright grey tone at O/Ti ~ 1.2 . Further increases of the O/Ti ratio induced the change of the film’s colour towards very dark grey tones, as revealed by the film with an atomic ratio O/Ti ~ 1.8 , where in fact the results indicate a transition from the metallic to the transition mode. In the transition zone, there is an inversion of the tendency for L^* to decrease. The plot shows a significant increase of this colorimetric coordinate, whose value increases from ~ 45 to 70. Slight increase in b^* and decrease in a^* were also observed. In the oxide zone, there was a clear tendency for the films to reveal interference colours, with very high values of L^* and very low values of both a^* and b^* . Anyway, and due to the interference-type tones, these colorimetric values need to be observed carefully. The overall behaviour can be explained by the decreasing metallic character of the films with the increasing O/Ti ratio and the transition towards a more insulating type represented by the oxide-type films prepared at the highest oxygen flows, see Fig. 2. The electron charge transfer from Ti atoms to O and C atoms increases with the increasing metalloid content in TiC_xO_y .

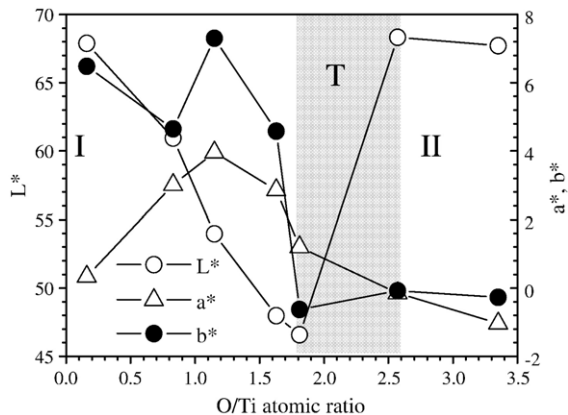


Fig. 3. Average colour coordinates in the CIELAB 1976 colour space under the standard CIE illuminant D_{65} , for films prepared with different O/Ti ratio.

The evolution of hardness, residual stresses and critical load as a function of the O/Ti ratio is shown in Fig. 4. Once again, the different structural changes have some effects on the mechanical properties evolution, where a significant reduction of hardness values is observed with the increase of the O/Ti ratio. The hardness ranges from typical values of TiC films for the lowest O/Ti ratio, to those of TiO_2 films for the highest O/Ti ratio [24,25]. The possibility of having a nanocomposite structure of the form nc-TiC(O)/a-C is consistent with the high hardness values obtained in the films located in zone I, as observed by researchers of recently published works [26,27]. The structural changes induced by the oxygen incorporation in the films seem to be the major responsibility of the decrease in hardness in zone T, resulting from the continuous amorphization tendency that is revealed in the films within this zone [28]. For the highest O/Ti ratios, there is a slight improvement of hardness, which might be related with the formation of poorly crystallized oxide phases (anatase and rutile).

Another fact that is worth to mention is the evolution of the residual stresses as a function of the O/Ti ratio. The plot shows that there is a significant reduction of stresses with the increase of the O/Ti ratio, indicating that the strain energy parameter is becoming less important than the surface free energy, which starts to prevail. For the $TiC_{1.6}(O)$ film, the high compressive stresses can be the result of the insertion of C atoms in the interstitial octahedral spaces of the host TiC matrix. The insertion of oxygen atoms in the TiC lattice can occur with the increase of the O/Ti ratio and might explain the almost amorphous nature of the existing TiC grains detected by XRD (see Fig. 2). Residual stresses can be correlated as well with the hardness values. From Fig. 4, it is clear that as the residual stresses decrease, the hardness suffers also a decrease, which means that beyond the different structural arrangements, the level of compressive residual stresses is also acting as a hardening factor.

Regarding the evolution of the adhesive critical loads (L_{C2} — first appearance of the substrate) as a function of the O/Ti ratio, it seems that once again the different structural changes occurring in the films are inducing different adhesion behaviours. In

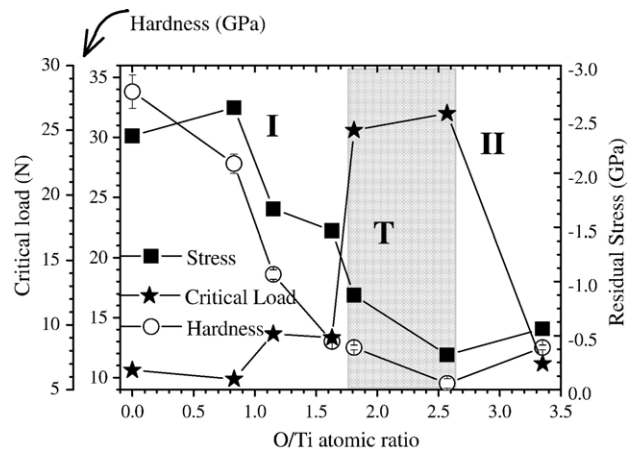


Fig. 4. Evolution of hardness, residual stresses and critical adhesion loads of sputtered TiC_xO_y films as a function of the O/Ti ratio.

fact, the highest critical loads occurred for films where the XRD results revealed amorphous structures, region T, which is understandable since these kinds of structures, are able to better accommodate the deformations induced by the movement of the scratch tip. Another point is related with the residual stresses states in the films. In fact, and taking into account the result obtained in region I and T, there seems to be some correlation between stresses and adhesion, since lower compressive stresses corresponded to higher critical adhesion loads. Nevertheless, these residual stress states are not able to alone explain all the behaviours since in the oxide region the stress levels are lower, but the critical adhesion loads are also significantly lower. If one keeps in mind that in this oxide region there is already some tendency to obtain poorly crystallized oxide structures, this means that the structural features are playing a decisive role for the adhesion behaviour.

Regarding the tribological characterization, it is worth to mention that TiC has been studied by many authors [29–31] and in this moment the main emphasis is given to the preparation of nc-TiC/a-C nanocomposite coatings [32]. On the other hand, it is known that Ti–O coatings have the possibility to form magnelis-phase (TiO_{2-x}), which is known to have very low friction coefficients. Taking this fact into account and also the possibility to form a nc-TiC phase and an amorphous phase (a-C or a-TiO_x), commonly observed in sputtered deposited films, induces that these TiC_xO_y films can be very good candidates for tribological applications. In this initial study of the tribological properties of TiC_xO_y coatings, only the static friction coefficient was studied, since this value is the highest value of the friction coefficient [33].

Fig. 5 shows the static friction coefficient for three different friction conditions, and the surface roughness as a function of the O/Ti ratio. It can be observed that for different friction conditions the results presented approximately the same trend, meaning that, for each sample, an increase in roughness of plane fixed half-couple (R_z between 0.4 and 2.5 μm), generally has no particular influence on the static friction coefficient. It is, however, worth to notice that there is a small tendency to have generally lower static friction coefficient for $R_z=2.5 \mu\text{m}$. This fact could be explained taking into account the number of

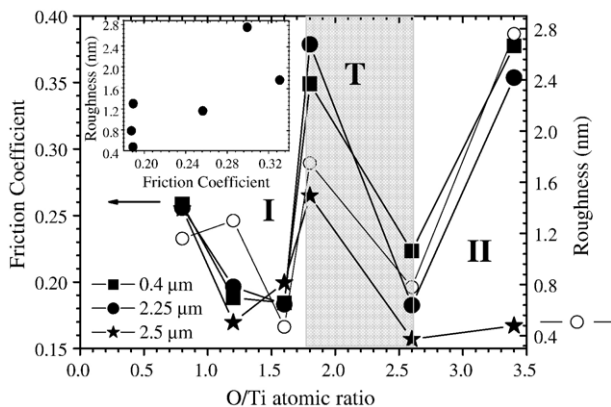


Fig. 5. Friction coefficient (solid symbols) and surface roughness (open circles) as a function of the O/Ti atomic ratio for three different friction conditions.

micro-contact bonds, which decrease if the roughness of plane fixed half-couple increases. At the same time, this aspect leads to a decrease of the adhesion force at the friction interface and the film removed often occurs earlier. For films within transition zone (O/Ti between 1.8 and 2.6), the static friction coefficient values presented a wide variation, and the samples revealed a very good tendency for sliding. Anyway, it is important to emphasize that, the results revealed that the static friction coefficient has no apparent correlation with the film's structure, since amorphous films (region T) and crystalline carbide and oxide ones (region I and II) have similar behaviours.

In this same Fig. 5, the samples' surface roughness is also plotted and by comparing its evolution with the variation of the static friction coefficient, upper left insert in Fig. 5, it seems that this is an important parameter to take into account. In fact, there seems to be some increase of the friction coefficients with the increase of the surface roughness. It is however important to note that this apparent correlation between film surface roughness and the tribological behaviour has to be taken very carefully, since there is a major influence coming from the counterbody roughness. In fact, one has to keep in mind that different scales of roughness of two different bodies are acting together: a film with nanometer scale roughness and a counterbody with micrometer scale roughness. Nevertheless, it is also obvious that the film roughness is changing (as well as the surface morphology) from one film to the other, while the roughness of the counterbody was kept approximately the same for all the films.

Furthermore, the results plotted in Fig. 4 shows also no direct correlation between the different mechanical characteristics and the tribological behaviour, and thus the different surface features are the main parameter to take into account for this variation of the friction coefficient.

4. Conclusions

TiC_xO_y thin films were deposited by dc reactive magnetron sputtering from a TiC target. The results showed that the evolution of the different film's properties are related to the 3 different growth regimes that were developed: a carbide zone (O/Ti ratio from 0.8 to 1.6); a transition zone (O/Ti ratios between 1.8 and 2.6), and an oxide one (O/Ti ratio higher than 3). There is a direct evident correlation between these regions and the film's composition evolution and the particular ratio of the elements.

The structural characterization showed that in the carbide regime the films crystallize in a TiC B1-NaCl-type crystal structure. In the transition regime, the films show a clear tendency towards amorphization, while a mixture of both poorly crystallized anatase and rutile TiO_2 phases is observed in the films prepared within the oxide zone.

A progressive reduction of hardness with the increase of the O/Ti ratio was observed, which was interpreted as the result of continuous amorphization of the films, with a slight increase in the oxide zone due to the formation of poorly crystallized oxide structures. The residual stresses presented also a decrease with the increase of the O/Ti ratio. The correlation between those properties means that the level of the compressive residual

stresses is acting as a hardening factor. The residual stresses are also playing an important role in the adhesion. Adhesion is enhanced with the decrease of the residual stresses, till the oxide region where a change of this behaviour is observed.

The surface roughness plays an important role on the static friction coefficient. However, there is no direct relation with the film's structure or with the mechanical properties.

Colour results indicate a strong influence of the O/Ti ratio on this property, which was found to be directly related with the structural changes.

Acknowledgments

The authors gratefully acknowledge the financial support of the Portuguese FCT Institution by the project no. POCTI/38086/CTM/2001 co-financed by European community fund FEDER.

References

- [1] I. Dahan, A. Admon, N. Frage, J. Sariel, M.P. Dariel, J.J. Moore, *Surf. Coat. Technol.* 137 (2001) 111.
- [2] A.A. Voevodin, M.A. Capano, S.J.P. Laube, M.S. Donley, J.S. Zabinski, *Thin Solid Films* 298 (1997) 107.
- [3] Y. Suda, H. Kawasaki, K. Doi, S. Hiraishi, *Thin Solid Films* 374 (2000) 282.
- [4] L.-Y. Kuo, P. Shen, *Mater. Sci. Eng., A Struct. Mater.: Prop. Microstruct. Process* 276 (2000) 99.
- [5] D. Chicot, Y. Benarioua, J. Lesage, *Thin Solid Films* 359 (2000) 228.
- [6] J. Kubarsepp, H. Klaasen, J. Pirso, *Wear* 249 (2001) 229.
- [7] K.E. Tan, A.M. Bratkovsky, R.M. Harris, A.P. Horsfield, D. Nguyen-Manh, D.G. Pettifort, A.P. Sutton, *Model. Simul. Mater. Sci. Eng.* 5 (1997) 187.
- [8] A.A. Adjaottor, E.I. Meletis, S. Logothetidis, I. Alexandrou, S. Kokkou, *Surf. Coat. Technol.* 76–77 (1995) 142.
- [9] F. Espinosa-Magaña, A. Duarte-Moller, R. Martínez-Sánchez, M. Miki-Yoshida, *J. Electron Spectrosc. Relat. Phenom.* 125 (2002) 119.
- [10] E. Kusano, A. Sato, N. Kikuchi, H. Nanto, A. Kinbara, *Surf. Coat. Technol.* 120–121 (1999) 378.
- [11] A.C. Fernandes, F. Vaz, L. Rebouta, A. Pinto, E. Alves, N.M.G. Parreira, Ph. Goudeau, E. Le Bourhis, J.P. Rivière, *Surf. Coat. Technol.* 201 (2007) 5587.
- [12] M. Nakamura, S. Kato, T. Aoki, L. Sirghi, Y. Hatanaka, *Thin Solid Films* 401 (2001) 138.
- [13] I. Yu Konyashin, *Thin Solid Films* 278 (1996) 37.
- [14] D.C. Kothari, M. Bonelli, A. Miottelo, L. Guzman, *Surf. Coat. Technol.* 100–101 (1998) 500.
- [15] E. Kusano, A. Sato, M. Kitagawa, H. Nanto, A. Kinbara, *Thin Solid Films* 343 (1999) 254.
- [16] *Colorimetry*, vol. 15, CIE Publ. (Commission Internationale de L'Éclairage), 1971.
- [17] Recommendations on Uniform Color Spaces, Difference–difference equations, psychometric color terms, CIE Publication, N° 2–70 (Commission Internationale de L'Éclairage) 15 (1978).
- [18] G.G. Stoney, *Proc. R. Soc. Lond.*, A 82 (1909) 172.
- [19] David A. Glocker, S. Ismat Shah, *Thin Film Process Technology*, Institute of Physics Publishing Ltd, Bristol, UK, 1995.
- [20] Powder Diffraction File, Joint Committee on Power Diffraction Standards, ASTM, Philadelphia, PA, 2000. Card 32–1383.
- [21] H. Liepack, K. Bartsch, W. Brückner, A. Leonhardt, *Surf. Coat. Technol.* 183 (2004) 69.
- [22] W. Precht, A. Czyzniewski, *Surf. Coat. Technol.* 174–175 (2003) 979.
- [23] A. Czyzniewski, W. Precht, *J. Mater. Process. Technol.* 157–158 (2004) 274.
- [24] A. Mani, P. Aubert, F. Mercier, H. Khodja, C. Berthier, P. Houdy, *Surf. Coat. Technol.* 194 (2005) 190.
- [25] M. Stüber, H. Leiste, S. Ulrich, H. Hollek, D. Schild, *Surf. Coat. Technol.* 150 (2002) 218.
- [26] T. Zehnder, J. Patscheider, *Surf. Coat. Technol.* 133–134 (2000) 133.
- [27] A. Leonhardt, H. Liepack, K. Bartsch, *Surf. Coat. Technol.* 133–134 (2000) 186.
- [28] W. Gulbiński, S. Mathur, H. Shen, T. Suszko, A. Gilewicz, B. Warcholiński, *Appl. Surf. Sci.* 239 (2005) 302.
- [29] L. Feng, J. Tang, J.S. Zabinski, *Mater. Sci. Eng., A Struct. Mater.: Prop. Microstruct. Process.* 257 (1998) 240.
- [30] Z. Yua, K. Inagawah, Z. Jin, *Thin Solid Films* 264 (1995) 52.
- [31] Y.Y. Guu, J.F. Lin, C. Ai, *Wear* 208 (1997) 147.
- [32] Y.T. Pei, D. Galvan, J.Th.M. De Hosson, C. Strondl, *J. Eur. Ceram. Soc.* 26 (2006) 565.
- [33] B.N.J. Persson, O. Albohr, F. Mancosu, V. Peveri, V.N. Samoilov, I.M. Sivebaek, *Wear* 254 (2003) 835.